

LinkGAN: Linking GAN Latents to Pixels for Controllable Image Synthesis

Jiapeng Zhu^{†*1} Ceyuan Yang^{†2} Yujun Shen^{†3} Zifan Shi^{*1} Deli Zhao⁴ Qifeng Chen¹
¹HKUST ²Shanghai AI Laboratory ³Ant Group ⁴Alibaba Group



Figure 1. **Precise local control** achieved by LinkGAN, where we can manipulate the image content within a spatial region (e.g., single eye or right half of the image) or a semantic category (e.g., car) simply by *resampling the latent code on same sparse axes*. Our approach works well with both 2D image synthesis, like StyleGAN2 [20] (left three columns), and 3D-aware image synthesis, like EG3D [4] (right two columns). It is noteworthy that, under the 3D-aware case, we can control both the appearance and the underlying geometry.

Abstract

This work presents an easy-to-use regularizer for GAN training, which helps explicitly link some axes of the latent space to an image region or a semantic category (e.g., sky) in the synthesis. Establishing such a connection facilitates a more convenient local control of GAN generation, where users can alter image content only within a spatial area simply by partially resampling the latent codes. Experimental results confirm four appealing properties of our regularizer, which we call **LinkGAN**. (1) Any image region can be linked to the latent space, even if the region is pre-selected before training and fixed for all instances. (2) Two or multiple regions can be independently linked to different latent axes, surprisingly allowing tokenized control of synthesized images. (3) Our regularizer can improve the spatial controllability of both 2D and 3D GAN models, barely sacrificing the synthesis performance. (4) The models trained with our regularizer are compatible with GAN inversion techniques and maintain editability on real images. Project page can be found [here](#).

[†] indicates equal contribution.

* This work was done during an internship at Ant Group.

1. Introduction

Generative adversarial networks (GANs) [10] have been shown to produce photo-realistic and highly diverse images, facilitating a wide range of real world applications [9, 15, 26, 31, 32]. The generator in a GAN is formulated to take a randomly sampled latent code as the input and output an image with a feed forward network. Given a well-learned GAN model, it is generally accepted that a variety of semantics and visual concepts automatically emerge in the latent space [12, 16, 33, 45, 51], which naturally support image manipulation. Some recent work also reveals the potential of GANs in local editing by steering the latent code along a plausible trajectory in the latent space [22, 50].

However, most studies on the relationship between the latent codes and their corresponding images depend on a posterior discovery, which usually suffers from three major drawbacks. (1) Instability: The identification of emerging latent semantics is very sensitive to the samples used for analysis, such that different samples may lead to different results [12, 32]. (2) Inaccuracy: Given the high-dimensional latent space (e.g., 512d in the popular StyleGAN family [19, 20]), finding a semantically meaningful subspace can be challenging. (3) Inflexibility: Existing manipulation models

are usually linear (*i.e.*, based on vector arithmetic [16, 32]), limiting the editing diversity.

This work offers a new perspective on learning controllable image synthesis. Instead of discovering the semantics from pre-trained GAN models, we introduce an efficient regularizer into the training of GANs, which is able to *explicitly* link some latent axes with an image region or a semantic category (*e.g.*, sky) in the synthesis, as shown in Fig. 2. In this way, the selected axes and the remaining axes are related to the in-region pixels and out-region pixels, respectively, with little cross-influence. Such a design, termed as **LinkGAN**, enables a more accurate and more convenient control of the generation, where we can alter the image content within the linked region simply by *resampling on the corresponding axes*.

We conduct experiments on various datasets to evaluate the efficacy of our approach and demonstrate its four appealing properties. (1) It is possible to link an arbitrary image region to the latent axes, no matter the region is pre-selected before training and fixed for all instances, or refers to a semantic category and varies across instances (see Sec. 4.2.1). (2) Our regularizer is capable of linking multiple regions to different sets of latent axes independently and simultaneously, and achieves joint manipulation of these regions. We even push the limit to tokenized image control (see Sec. 4.2.2). (3) Our approach lends itself well to both 2D image synthesis models [20] and 3D-aware image synthesis models [4], by sufficiently improving the controllability yet barely harming the synthesis performance (see Fig. 1). (4) The models trained with our regularizer are compatible with GAN inversion techniques [52] and maintain the editability on real images (see Sec. 4.3). We believe that this work makes a big step towards the spatial controllability of GANs as well as the explicit disentanglement of GAN latent space.

2. Related Work

Generative adversarial networks. Generative adversarial networks (GANs) are composited by a generator and a discriminator, which are trained simultaneously by playing a two-player minimax game [10], have made tremendous progress in generating high quality and diversity images [3, 18–20, 44]. In turn, there are widely used in a variety of tasks, such as representation learning [17, 43], image-to-image translation [6, 15], image segmentation [48], image editing [5, 22, 32], 3D generation [4, 34, 42] *etc.*

Semantic discovery in GANs. Interpreting the pre-trained GANs [1, 2, 32] has drawn lots of attention recently since it will help us to understand how an image in GANs is rendered, which in turn, enables us to control the generation process of the GANs. Many recent works [7, 12, 32, 38, 50] have demonstrated the latent space of GANs encodes rich semantic information that can be used to edit the

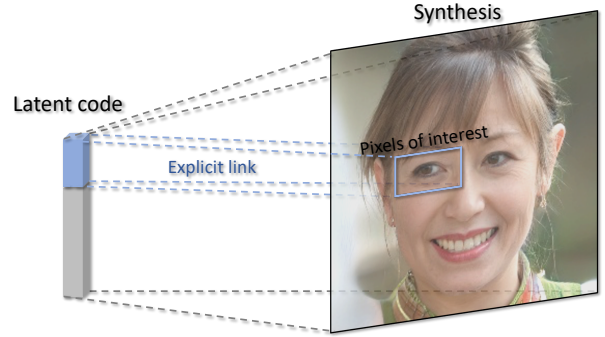


Figure 2. **Concept diagram** of LinkGAN, where some axes of the latent space are *explicitly* linked to the image pixels of a spatial area. In this way, we can alter the image content within the linked region simply by resampling the latent code on these axes.

output images globally or locally by merely shifting the corresponding latent codes. For the methods that control the output images globally [5, 12, 16, 21, 29, 32, 33, 36, 38, 39, 45, 47], they either use some off-shell classifiers to find the variation of factors supervised or just find them unsupervised. For the methods that control the output images locally [1, 2, 7, 22, 37, 41, 43, 50, 51], they either control from the feature maps [2, 37, 43], control from weights of the generator [1], or control from the latent space [7, 22, 41, 50, 51]. However, all of these works try to interpret the pre-trained GANs, but few of them apply those findings during GAN training.

Regularizers for GAN training. Many attempts have been made to regularize GANs during training [11, 13, 20, 23, 28, 35, 40, 44]. Some of them try to improve the training stability of GANs by regularizing the gradients of the discriminator [11, 23], the spectral norm of each layer [24], or the singular values of the generator [25]. Besides, some of them [8, 13, 20, 28, 35, 40] aim to improve the disentanglement property of GANs. For example, [28, 40] try to disentangle each component in the latent vectors so that each dimension in the latent codes can only affect one attribute on the output images by adding some regularizers (*e.g.*, Hessian Penalty or Orthogonal Jacobian Regularization). In StyleGAN2 [20], a path length regularization is added to encourage the learned generator to become much smoother. And [8, 35] try to disentangle different semantics in the latent space by borrowing some labels. But none of them tries to relate an arbitrary region to a specific latent part.

3. Method

In this section, we first give some background knowledge regarding GANs as well as the conventional manipulation model using GANs in Sec. 3.1. Our method that bridges specified subspaces of the whole latent space with a parti-

tion of a synthesized image is presented in Sec. 3.2.

3.1. Preliminaries

A **generative adversarial network (GAN)** consists of a generator $G(\cdot)$ that maps latent vectors $z \sim p(z)$ to fake images, *i.e.*, $\tilde{x} = G(z)$, and a discriminator $D(\cdot)$ that tries to differentiate fake images from real ones. They are trained in an adversarial manner, in the sense that the generator tries to fool the discriminator while the discriminator learns to measure the realness of generated images. The training loss can be formulated as follows:

$$\mathcal{L}_G = \mathbb{E}_{p(\tilde{x})}[f(1 - D(\tilde{x}))], \quad (1)$$

$$\mathcal{L}_D = \mathbb{E}_{p(x)}[f(D(x))] - \mathbb{E}_{p(\tilde{x})}[f(1 - D(\tilde{x}))], \quad (2)$$

where $p(x)$ and $p(\tilde{x})$ are the distributions of real images and synthesized images, respectively. Besides, f is a model-specific function that varies between different GANs.

Conventional manipulation leverages a pre-trained GAN for content editing since many prior arts [30, 32] have shown that the latent space of a GAN is correlated with the property of semantic arithmetic. For instance, adding or removing the glass from an image can be fulfilled by performing simple additive or subtractive operations in the latent space. The manipulation model can be formulated as follows:

$$x^{\text{edit}} = G(z + \alpha n), \quad (3)$$

where n is the attribute vector in the latent space and α is the step for the manipulation. In other words, when a latent code is moved toward the attribute vector, the corresponding attribute contained in the output image will vary accordingly. Notably, such a manipulation strategy tends to modify global attributes of synthesis.

3.2. Linking Latents to Pixels

With the rapid development of manipulation technique, several works [22, 50] have shown that some subspaces of the latent space (*i.e.*, the w space in StyleGAN [19]) can control local semantics over output images. Specifically, traversing a latent code within those subspaces results in a local modification in the synthesis. However, there lacks an explicit connection between the local regions and the specified axes of latent spaces. To this end, we propose a new regularizer explicitly linking the axes to arbitrary partitions of synthesized images.

Partition of latent codes and images. In order to set up the explicit link between some axes of latent space and local regions of an image, we first introduce some notations for the corresponding partition. Taking StyleGAN [19] as an example, $w \in \mathbb{R}^{d_w}$ is the intermediate latent vector of dimension d_w derived from the mapping network. Through a generator $G(\cdot)$, an image $\tilde{x} \in \mathbb{R}^{d_x}$ with dimension d_x

is produced, *i.e.*, $\tilde{x} = G(w)$. Note that here the image in editing is reshaped as a vector for brevity. Namely, the dimension d_x is equal to the multiplication between the width and height of images (the color channels are also neglected here).

We first divide the latent space into several subspaces. Namely, a latent code w could be divided into K fragments *i.e.*, $w = [w_1, w_2, \dots, w_K]$, where one partition w_i consists of multiple channels $w_i = [w_{i1}, w_{i2}, \dots, w_{in_i}]$ and $\sum_{i=1}^K n_i = d_w$. Similarly, an image \tilde{x} could also produce several partitions *i.e.*, $\tilde{x} = [\tilde{x}_1, \tilde{x}_2, \dots, \tilde{x}_K]$, where $\tilde{x}_i \in \mathbb{R}^{m_i}$ and $\sum_{i=1}^K m_i = d_x$. Importantly, we further define w_i^c and \tilde{x}_i^c are the complements of w_i and \tilde{x}_i , respectively, *i.e.*, $w_i^c = [w_1, \dots, w_{i-1}, w_{i+1}, \dots, w_K]$, $\tilde{x}_i^c = [\tilde{x}_1, \dots, \tilde{x}_{i-1}, \tilde{x}_{i+1}, \dots, \tilde{x}_K]$. Fig. 2 presents an example (K is equal to 2) where the blue part of the latent code and pixels within the blue bounding box denote the partitions w_i and \tilde{x}_i , respectively. Now, our goal is that the latent fragment w_i only controls the pixels in \tilde{x}_i and w_i^c controls the pixels in \tilde{x}_i^c , namely, building an explicit link illustrated in Fig. 2.

Learning objectives. To our surprise, we find in practice that a simple regularizer combined with the StyleGAN framework is sufficient to achieve this goal. Formally, we can randomly perturb w_i and w_i^c and then minimize the variations on \tilde{x}_i^c and \tilde{x}_i , respectively, expecting that w_i merely controls \tilde{x}_i and hardly affects \tilde{x}_i^c and vice versa.

To be specific, we use two vectors p and \bar{p} to perturb w_i and w_i^c , respectively, where $p = [0, \dots, 0, p_i, 0, \dots, 0]$, $\bar{p} = [p_1, \dots, p_{i-1}, 0, p_{i+1}, \dots, p_K]$, and each non-zero sub-vector in p and \bar{p} is sampled from a standard Gaussian distribution $\mathcal{N}(0, I)$. Thus we can obtain two perturbed images, *i.e.*, $\tilde{x}_1 = G(w + \alpha p)$ and $\tilde{x}_2 = G(w + \alpha \bar{p})$ regarding the original one \tilde{x} . The pixel change in \tilde{x}_i^c after the perturbation by p can be computed as

$$\mathcal{L}_1 = \|M_1 \odot (\tilde{x}_1 - \tilde{x})\|_2^2 = \|M_1 \odot (G(w + \alpha p) - G(w))\|_2^2, \quad (4)$$

where M_1 is the binary mask denoting the region out of interest, $\|\cdot\|_2$ denotes the ℓ_2 norm, and α is the perturbation strength. We want the pixels to change in the region \tilde{x}_i^c as minimally as possible after the perturbation by p . Similarly, the pixels change in \tilde{x}_i after the perturbation by \bar{p} can be written as

$$\mathcal{L}_2 = \|M_2 \odot (\tilde{x}_2 - \tilde{x})\|_2^2 = \|M_2 \odot (G(w + \alpha \bar{p}) - G(w))\|_2^2, \quad (5)$$

where M_2 is the binary mask indicating the chosen pixels of interest. These two losses \mathcal{L}_1 and \mathcal{L}_2 can be integrated as a regularizer in the StyleGAN framework.

$$\mathcal{L}_{reg} = \lambda_1 \mathcal{L}_1 + \lambda_2 \mathcal{L}_2, \quad (6)$$

where λ_1 and λ_2 are the weights to balance these two terms. Therefore, the total loss to train the generator in StyleGAN

can be formulated as

$$\mathcal{L} = \mathcal{L}_G + \mathcal{L}_{reg}. \quad (7)$$

Practically, we could apply the new regularization \mathcal{L}_{reg} in a lazy way, in the sense that \mathcal{L}_{reg} is calculated once every several iterations (8 iterations in this paper), greatly improving the training efficiency. Additionally, the perturbed images would be also fed into the discriminator during training. Noticeably, Eq. (6) gives the regularization loss on how to build one explicit link, if we want to build multiple links between image regions and latent fragments, we need to compute \mathcal{L}_{reg} on each link and sum them all, *i.e.*, $\sum_{j=1}^k \mathcal{L}_{reg}^j$, where k ($1 \leq k \leq K$) is the number of links we want to build.

4. Experiments

4.1. Experimental Setup

We conduct extensive experiments to evaluate our proposed method. We mainly conduct our experiment on StyleGAN2 [20] and EG3D [4] models. The datasets we use are FFHQ [19], AFHQ [6], LSUN-Church, LSUN-Car [46]. We also use a segmentation model [49] to select pixels with the same semantic (*e.g.*, all the pixels in the sky on LSUN-Church). The main metrics we use to qualify our method are Fréchet Inception Distance (FID) [14] and the masked Mean Squared Error (MSE) [50]. The experiments are organized as follows. First, Sec. 4.2 shows the properties of LinkGAN, which can relate an arbitrary region in the image to the latent fragment. Second, Sec. 4.3 gives some applications of our method, such as local control on the 3D generative model, real images, and some comparisons with the baselines regarding the editing precision. At last, Sec. 4.4 presents an ablation study on the size of the link latent subspace.

4.2. Properties of LinkGAN

In this section, we mainly demonstrate the effectiveness of the proposed approach by explicitly linking the pixels in any region (both the single region or multi-regions) to a partition of the corresponding latent codes, while seldom deteriorating the quality of synthesis. Tab. 1 reports FID on different datasets when our regularizer is added, from which we can see our regularizer only has a minor influence on the synthesized quality. Empirically, we find that it would more stable if the proposed regularizer is incorporated after the convergence of the generator. Therefore, we start training from a relatively well-trained generator and equipping it with our approach.

4.2.1 Linking Latents to Single Region

Regarding the partition of latent codes, we could easily choose the first several channels as one group. Accord-

Table 1. Performance change after introducing our proposed regularizer into 2D and 3D baselines, where the synthesis quality slightly drops but the controllability significantly improves (see Figs. 3 to 6 for details).

	StyleGAN2 [20]				EG3D [4]
Dataset	FFHQ	AFHQ	Car	Church	FFHQ
Baseline	3.98	7.92	2.95	3.82	4.28
LinkGAN (ours)	5.11	10.2	3.50	4.59	4.67

ingly, the remaining ones become the complementary code. Therefore, the goal of the proposed regularizer is to enable the explicit control of certain regions of interest through the chosen channels. Note that the number of first channels that would be grouped usually depends on the area ratio of the chosen region over the entire image. In the following context, we will show different ways of choosing pixels out of images and building explicit links between the chosen channels and pixels.

Region-based control. One general way of grouping pixels is to use a bounding box that could cover a rectangle region. Fig. 3 presents the qualitative results of choosing different regions randomly. Red bounding boxes in Fig. 3 denote the chosen regions of interest. In terms of human faces on FFHQ, we randomly select two spatial patches that usually contain either complicated or non-special semantics (*e.g.*, half of faces or just a cube of background). Obviously, after building the explicit link, we could merely change the chosen regions by perturbing the corresponding partition of latent codes, while maintaining the rest regions untouched. Besides, perturbing the complementary latent codes results in substantial change for regions out of interest, demonstrating that the spatial controlling is well-built by the proposed explicit link. Additionally, we also verify the effectiveness of our regularizer on various datasets. For instance, the connection between a partition of latent code and two eyes or one ear of animal faces could be also easily set up, causing appealing editing results. Moreover, not only a relatively small region but also the larger one could be well linked to several axes of latent space. Results on LSUN Church suggest that even half of the entire image is also controllable with the aid of the proposed approach. The difference maps further present how well such an explicit link could control a region of interest.

Semantic-based control. Prior experimental results demonstrate the control on a rectangle region that seems to be irrelevant to a certain visual concept. Namely, this link is semantic-agnostic since it merely bridges several channels with spatial locations rather than semantics. Therefore, we further conduct experiments on semantic controlling. To be specific, by leveraging an off-the-shelf segmentation model [49], we could easily obtain mask annotations that specify various semantics.

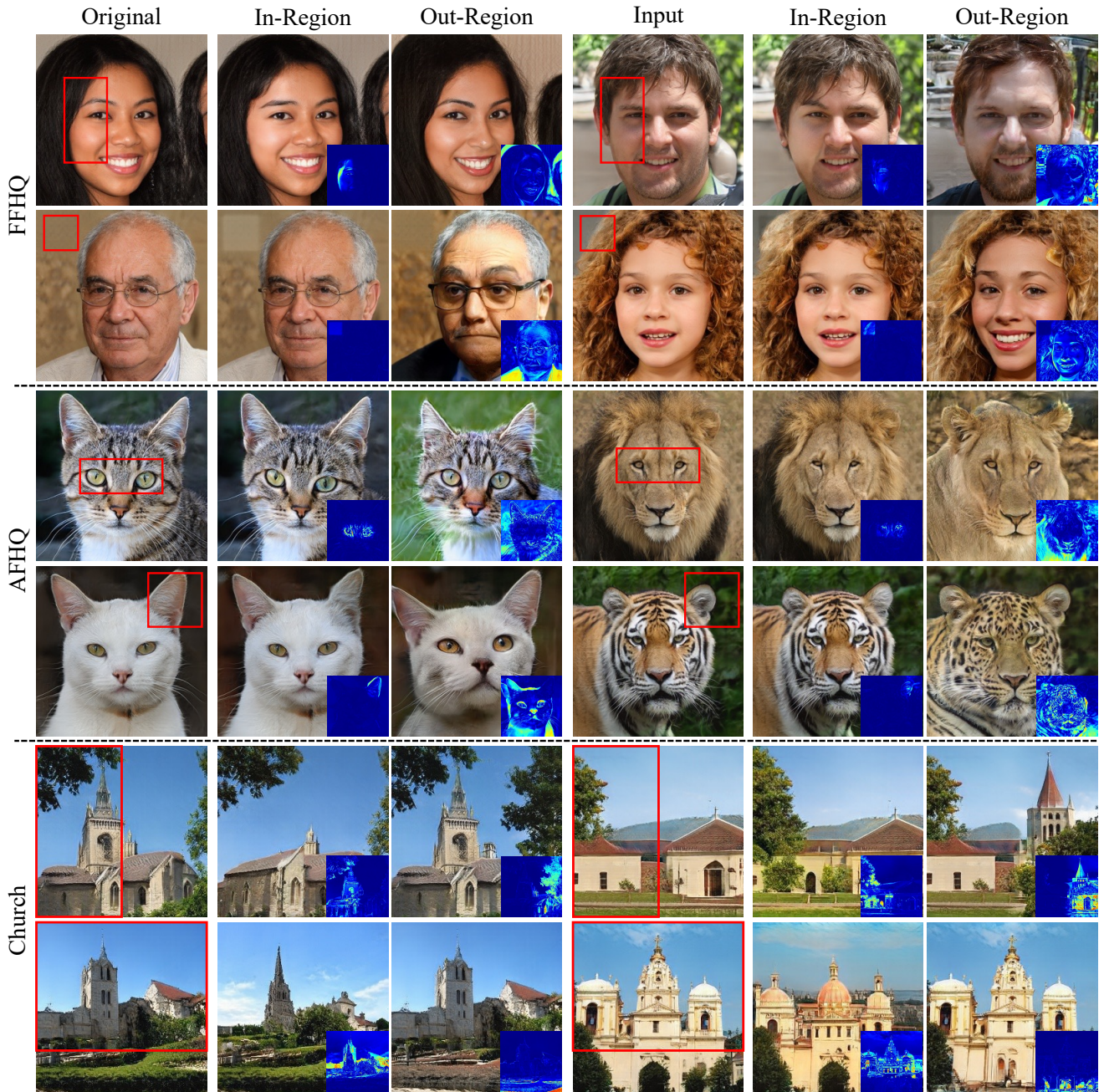


Figure 3. **Linking latents to single fixed region**, which is pre-selected before training and shared by all instances. Linked regions are highlighted with red boxes, and the heatmaps reflect the change of pixel values after in-region resampling and out-region resampling. We find that LinkGAN can robustly link the latents to an arbitrary image region, even semantically meaningless ones (e.g., the second row).

Fig. 4 presents the semantic control on two datasets, LSUN-Church and LSUN-Car [46]. In particular, churches and cars are chosen as the semantics that we would like to build a link between latent space to, no matter where the chosen semantics are. Similarly, we manage to connect several channels of latent space with a given semantic such that perturbing the chosen channels will result in the

obvious change of semantics. For instance, the color and shape of a church vary while the sky keeps the same and vice versa. Regarding the experiments on cars, the color could be modified no matter what cars face and how many pixels cars occupy. All these results together with the rectangle region control demonstrate the arbitrary region control enabled by our approach.

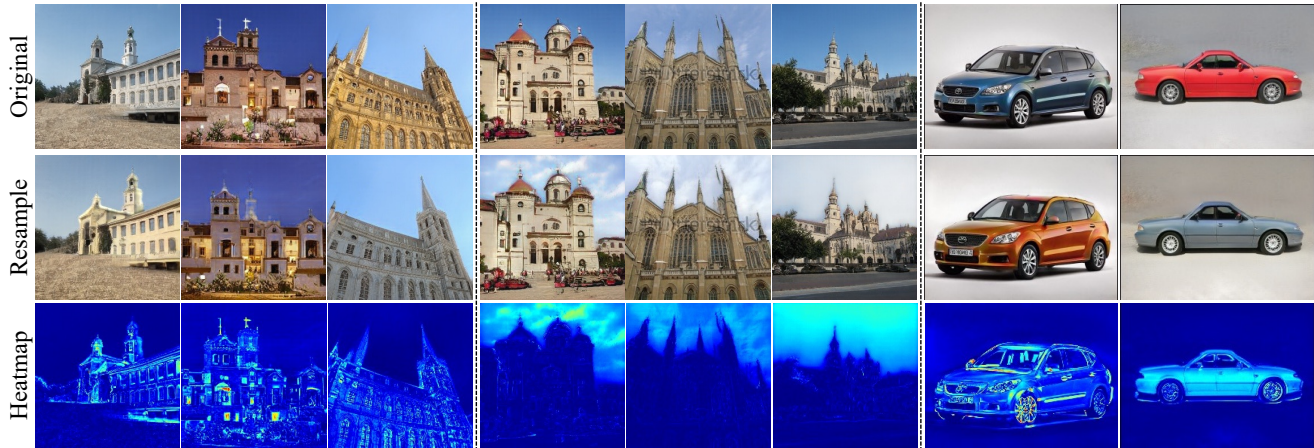


Figure 4. **Linking latents to semantic region** (*i.e.*, church, sky, and car) which dynamically varies across instances. Our LinkGAN manages to precisely control a particular semantic category simply by resampling on some sparse latent axes.

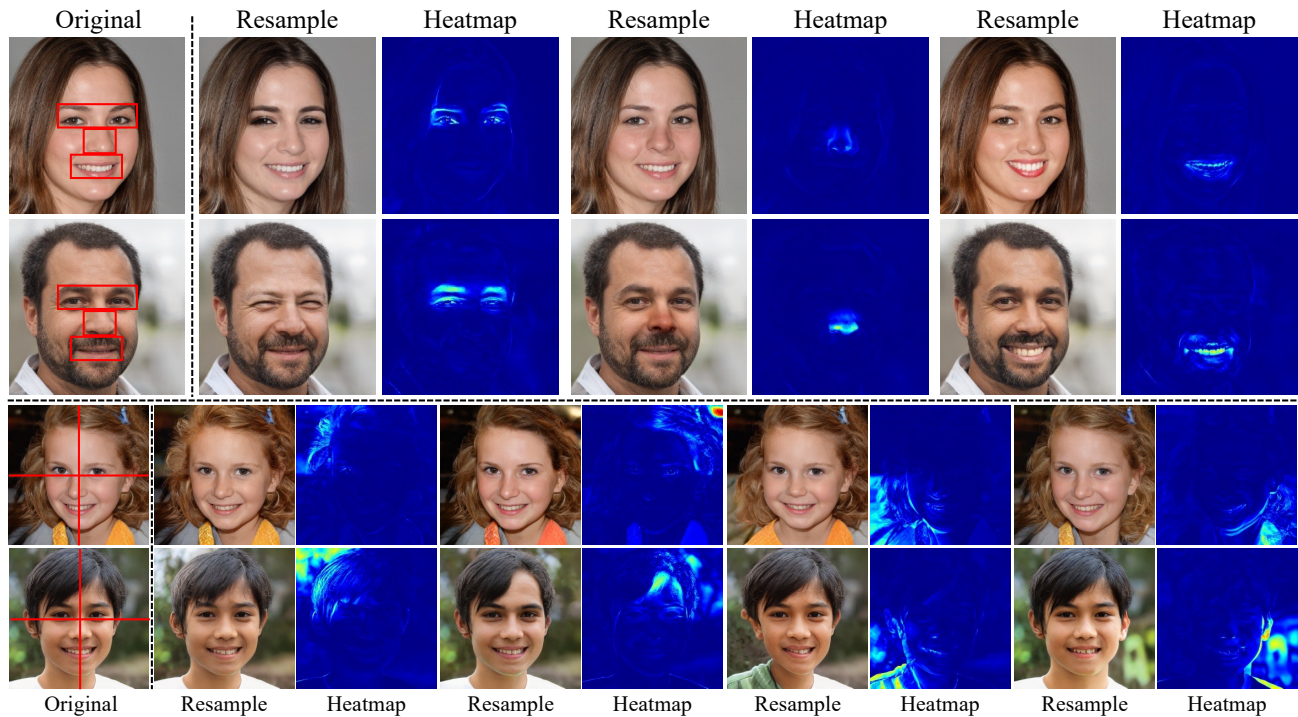


Figure 5. **Linking latents to multiple regions**, where the regions highlighted by red boxes are simultaneously linked to some non-overlapping sets of latent axes and can be independently controlled by partially resampling the latent codes. We even achieve tokenized control of the synthesis as shown below.

4.2.2 Linking Latents to Multiple Regions

After checking the effectiveness of our approach on building one explicit link, a natural question then arises: is it possible to link multiple regions of interest to multiple partitions of latent codes?

Joint control. Fig. 5 presents the corresponding results. On top of that, we link three subspaces that contain 64 channels to three image regions *i.e.*, eye, nose, and mouth, respectively. Even though we could remain to manipulate

semantics individually.

Tokenized control. The bottom one moves forward to a more challenging setting that both latent spaces and images are equally divided into four groups and four corners without any overlap. To this end, we could tell that such a regularizer could build a full explicit link between the entire latent space and the whole synthesis in a disentangled way. Namely, we can even tokenize an image and assign one subspace to each token.



Figure 6. **Controllability on 3D-aware generative model**, *i.e.*, EG3D [4], under the cases of mouth and nose. We find that LinkGAN is well compatible with 3D-aware image synthesis and allows controlling both the appearance and the underlying geometry.

4.3. Applications of LinkGAN

In this part, we show that our proposed method can be used in various applications, such as controlling 3D generative models, real image manipulation, and precise local image editing, *etc.*

Towards 3D-aware generation. We implement our regularizer on the 3D generative model EG3D [4]. Surprisingly, our regularizer performs well not only in controlling the RGB images but also in controlling the geometry of the corresponding image, showing the good generalization ability of our regularizer. Fig. 6 shows the results of controlling the mouth and nose region by perturbing the first 64 channels of latent codes. Importantly, controlling the linked subspace simultaneously changes the RGB images and their geometry, *i.e.*, mouth is opening for both RGB and corresponding 3D geometry.

Real image editing. After the generator is trained, we can use the property of the trained generator to control real images locally by inversion [20, 52]. Fig. 7 shows the editing results on the real image, in which the eyes can be independently controlled, *i.e.*, we can only open one eye yet keep another eye untouched. In this case, we need to explicitly link two eye regions to two latent subspaces, *i.e.*, one subspace controls one eye. And when the generator is well-learned, we can edit the eye region by controlling the corresponding subspace on the inverted latent code.

Comparison with existing methods. Now we compare our method with some state-of-the-art algorithms (*e.g.*, ReSeFa [51]) regarding local control precision. As shown in Fig. 8, we can observe that our method can reach more precise control on the local regions than ReSeFa. For instance, when modifying eyes, ReSeFa also results in a change of face color. On the contrary, when editing the specific region, our method has negligible changes in the other regions. Tab. 2 reports the masked MSE between our method and ReSeFa when controlling those three regions.

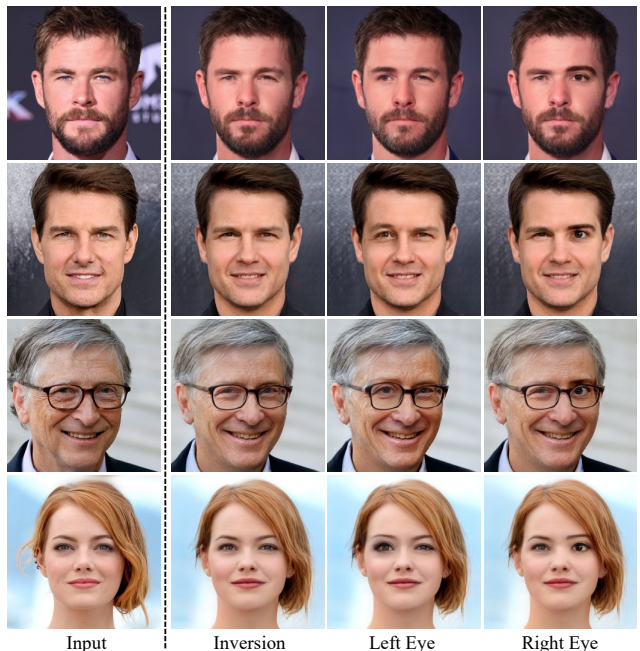


Figure 7. **Real image editing** achieved by LinkGAN via borrowing the GAN inversion technique [20]. We manage to edit the two eyes of human independently in a very convenient way, *i.e.*, partially resampling the inverted code.

Namely, when editing a specific region, we want the change in this region to be as larger as possible (the higher MSE, the better) and the change in the remaining region as small as possible (the smaller MSE, the better). We can observe that the MSEs within the edited regions are comparable. However, regarding the MSEs out of the edited regions, our method significantly outperforms ReSeFa.

4.4. Ablation Study on Linking Dimensionality

In this part, we conduct an ablation study on how many axes are required to build an explicit link. Eyes

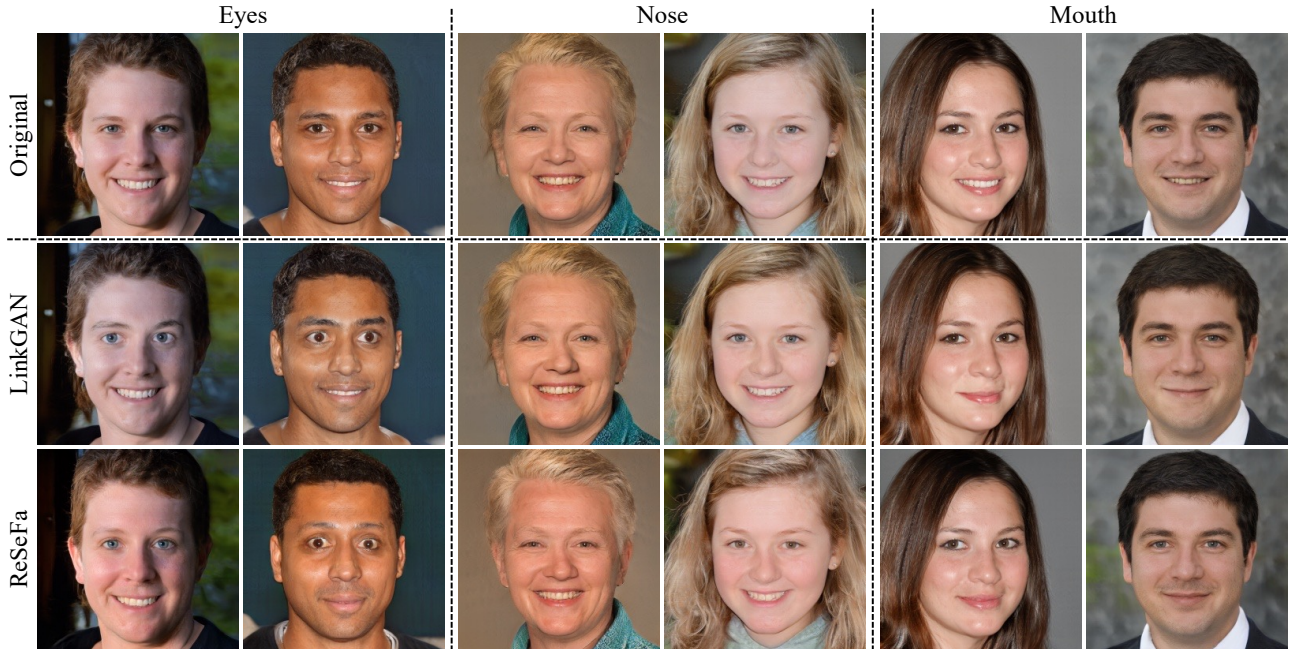


Figure 8. **Qualitative comparison** with ReSeFa [51], which posteriorly discovers semantics from a pre-trained model, on the task of local editing. LinkGAN achieves more precise control within the regions of interest. See Tab. 2 for quantitative results.

Table 2. **Quantitative comparison** with ReSeFa [51] on the task of local editing. Pixel-wise mean square error (MSE) *within/out* of the region of interest (scaled by $1e^{-3}$ for better readability) is used as the metric. Lower MSE_o and higher MSE_i are better.

Region	Eyes		Nose		Mouth	
	MSE_i	MSE_o	MSE_i	MSE_o	MSE_i	MSE_o
ReSeFa [51]	5.90	61.14	1.12	60.4	2.02	50.55
LinkGAN (ours)	5.25	2.24	1.82	2.25	3.10	2.21

of faces are chosen as regions of interest. Tab. 3 gives the quantitative results of changing in/out eye regions with the same perturbation strength. In Tab. 3, all the training configurations are the same except for the number of axes during training. MSE_i and MSE_o are computed in and out of the eye region when perturbing on their complementary latent space, respectively. Take axes number 8 as an example, and the MSE_i is computed within the eye region when perturbing on axes from 8 to 512, while MSE_o is computed out of the eye region perturbing on axes from 0 to 8. In such a way, precise control could be obtained since the perturbing on the complementary latent space should barely influence the regions of interest. Hence, in this situation, both MSE_i and MSE_o are the smaller, the better. Obviously, when occupying the first 64 axes, we can get satisfying results since the sum of them is the smallest. In practice, we set the number of axes in latent code to 64 in most cases, such as when controlling on eyes, nose, mouth, etc. And the detailed axes for other datasets can be found in *Appendix*.

Table 3. **Ablation study** on the linking dimensionality. MSE_i measures the effect of unlinked axes on the linked region, while MSE_o measures the effect of linked axes on the unlinked region, both of which enjoy a small value. All numbers are scaled by $1e^{-3}$ for better readability.

# Linked axes	8	16	32	64	128	256
MSE_i	17.45	16.70	3.29	0.95	0.78	0.43
MSE_o	0.86	1.53	7.41	8.20	8.71	24.78

5. Discussion and Conclusion

After linking an arbitrary region to some latent axes with the size of n , any perturbation with randomly sampled n dimension vector on the linked subspace results in the content change only in the linked image region, which can be viewed as a local semantic direction since it only influences the linked region. However, some of the sampled latent vectors can not generate realistic manipulation, and some of them can. Hence, we need to verify whether the randomly sampled vector can produce a meaningful manipulation posteriorly, just like other unsupervised methods [12, 33].

In this work, LinkGAN is proposed to explicitly link some latent axes to a region of an image or a semantic by utilizing an easy yet powerful regularizer. Extensive experiments demonstrate the powerful ability to precisely control the synthesized image locally from the linked latent subspace.

References

- [1] David Bau, Steven Liu, Tongzhou Wang, Jun-Yan Zhu, and Antonio Torralba. Rewriting a deep generative model. In *Eur. Conf. Comput. Vis.*, 2020. 2
- [2] David Bau, Jun-Yan Zhu, Hendrik Strobelt, Bolei Zhou, Joshua B. Tenenbaum, William T. Freeman, and Antonio Torralba. GAN dissection: Visualizing and understanding generative adversarial networks. In *Int. Conf. Learn. Represent.*, 2019. 2
- [3] Andrew Brock, Jeff Donahue, and Karen Simonyan. Large scale GAN training for high fidelity natural image synthesis. In *Int. Conf. Learn. Represent.*, 2019. 2
- [4] Eric R. Chan, Connor Z. Lin, Matthew A. Chan, Koki Nagano, Boxiao Pan, Shalini De Mello, Orazio Gallo, Leonidas Guibas, Jonathan Tremblay, Sameh Khamis, Tero Karras, and Gordon Wetzstein. Efficient geometry-aware 3D generative adversarial networks. In *IEEE Conf. Comput. Vis. Pattern Recog.*, 2022. 1, 2, 4, 7, 11
- [5] Anton Cherepkov, Andrey Voynov, and Artem Babenko. Navigating the GAN parameter space for semantic image editing. In *IEEE Conf. Comput. Vis. Pattern Recog.*, 2021. 2
- [6] Yunjey Choi, Youngjung Uh, Jaejun Yoo, and Jung-Woo Ha. StarGAN v2: Diverse image synthesis for multiple domains. In *IEEE Conf. Comput. Vis. Pattern Recog.*, 2020. 2, 4, 11
- [7] Edo Collins, Raja Bala, Bob Price, and Sabine Susstrunk. Editing in style: Uncovering the local semantics of GANs. In *IEEE Conf. Comput. Vis. Pattern Recog.*, 2020. 2
- [8] Chris Donahue, Zachary C Lipton, Akshay Balsubramani, and Julian McAuley. Semantically decomposing the latent spaces of generative adversarial networks. *Int. Conf. Learn. Represent.*, 2018. 2
- [9] Patrick Esser, Robin Rombach, and Bjorn Ommer. Taming transformers for high-resolution image synthesis. In *IEEE Conf. Comput. Vis. Pattern Recog.*, 2021. 1
- [10] Ian Goodfellow, Jean Pouget-Abadie, Mehdi Mirza, Bing Xu, David Warde-Farley, Sherjil Ozair, Aaron Courville, and Yoshua Bengio. Generative adversarial nets. In *Adv. Neural Inform. Process. Syst.*, 2014. 1, 2
- [11] Ishaan Gulrajani, Faruk Ahmed, Martin Arjovsky, Vincent Dumoulin, and Aaron C Courville. Improved training of wasserstein GANs. In *Adv. Neural Inform. Process. Syst.*, 2017. 2
- [12] Erik Härkönen, Aaron Hertzmann, Jaakko Lehtinen, and Sylvain Paris. GANSpace: Discovering interpretable GAN controls. In *NeurIPS*, 2020. 1, 2, 8
- [13] Zhenliang He, Meina Kan, and Shiguang Shan. EigenGAN: Layer-wise eigen-learning for GANs. In *Int. Conf. Comput. Vis.*, 2021. 2
- [14] Martin Heusel, Hubert Ramsauer, Thomas Unterthiner, Bernhard Nessler, and Sepp Hochreiter. GANs trained by a two time-scale update rule converge to a local nash equilibrium. In *Adv. Neural Inform. Process. Syst.*, 2017. 4
- [15] Phillip Isola, Jun-Yan Zhu, Tinghui Zhou, and Alexei A Efros. Image-to-image translation with conditional adversarial networks. *IEEE Conf. Comput. Vis. Pattern Recog.*, 2017. 1, 2
- [16] Ali Jaharian, Lucy Chai, and Phillip Isola. On the "steerability" of generative adversarial networks. *arXiv preprint arXiv:1907.07171*, 2019. 1, 2
- [17] Donahue Jeff and Simonyan Karen. Large scale adversarial representation learning. In *Adv. Neural Inform. Process. Syst.*, 2019. 2
- [18] Tero Karras, Miika Aittala, Samuli Laine, Erik Härkönen, Janne Hellsten, Jaakko Lehtinen, and Timo Aila. Alias-free generative adversarial networks. In *Adv. Neural Inform. Process. Syst.*, 2021. 2
- [19] Tero Karras, Samuli Laine, and Timo Aila. A style-based generator architecture for generative adversarial networks. In *IEEE Conf. Comput. Vis. Pattern Recog.*, 2019. 1, 2, 3, 4
- [20] Tero Karras, Samuli Laine, Miika Aittala, Janne Hellsten, Jaakko Lehtinen, and Timo Aila. Analyzing and improving the image quality of StyleGAN. In *IEEE Conf. Comput. Vis. Pattern Recog.*, 2020. 1, 2, 4, 7, 11
- [21] Xiao Li, Chenghua Lin, Ruizhe Li, Chaozheng Wang, and Frank Guerin. Latent space factorisation and manipulation via matrix subspace projection. In *Int. Conf. Mach. Learn.*, 2020. 2
- [22] Huan Ling, Karsten Kreis, Daiqing Li, Seung Wook Kim, Antonio Torralba, and Sanja Fidler. EditGAN: High-precision semantic image editing. In *Adv. Neural Inform. Process. Syst.*, 2021. 1, 2, 3
- [23] Lars Mescheder, Sebastian Nowozin, and Andreas Geiger. Which training methods for GANs do actually converge? In *Int. Conf. Mach. Learn.*, 2018. 2
- [24] Takeru Miyato, Toshiki Kataoka, Masanori Koyama, and Yuichi Yoshida. Spectral normalization for generative adversarial networks. *Int. Conf. Learn. Represent.*, 2018. 2
- [25] Augustus Odena, Jacob Buckman, Catherine Olsson, Tom Brown, Christopher Olah, Colin Raffel, and Ian Goodfellow. Is generator conditioning causally related to GAN performance? In *Int. Conf. Mach. Learn.*, 2018. 2
- [26] Taesung Park, Ming-Yu Liu, Ting-Chun Wang, and Jun-Yan Zhu. Semantic image synthesis with spatially-adaptive normalization. In *IEEE Conf. Comput. Vis. Pattern Recog.*, 2019. 1
- [27] Or Patashnik, Zongze Wu, Eli Shechtman, Daniel Cohen-Or, and Dani Lischinski. StyleCLIP: Text-driven manipulation of StyleGAN imagery. In *Int. Conf. Comput. Vis.*, 2021. 11, 12, 13
- [28] William Peebles, John Peebles, Jun-Yan Zhu, Alexei A. Efros, and Antonio Torralba. The hessian penalty: A weak prior for unsupervised disentanglement. In *Eur. Conf. Comput. Vis.*, 2020. 2
- [29] Antoine Plummerault, Hervé Le Borgne, and Céline Hudelot. Controlling generative models with continuous factors of variations. In *Int. Conf. Learn. Represent.*, 2020. 2
- [30] Alec Radford, Luke Metz, and Soumith Chintala. Unsupervised representation learning with deep convolutional generative adversarial networks. In *Int. Conf. Learn. Represent.*, 2016. 3

- [31] Aditya Ramesh, Mikhail Pavlov, Gabriel Goh, Scott Gray, Chelsea Voss, Alec Radford, Mark Chen, and Ilya Sutskever. Zero-shot text-to-image generation. In *Int. Conf. Mach. Learn.*, 2021. 1
- [32] Yujun Shen, Ceyuan Yang, Xiaoou Tang, and Bolei Zhou. InterFaceGAN: Interpreting the disentangled face representation learned by GANs. *IEEE Trans. Pattern Anal. Mach. Intell.*, 2020. 1, 2, 3
- [33] Yujun Shen and Bolei Zhou. Closed-form factorization of latent semantics in GANs. In *IEEE Conf. Comput. Vis. Pattern Recog.*, 2021. 1, 2, 8
- [34] Zifan Shi, Yujun Shen, Jiapeng Zhu, Dit-Yan Yeung, and Qifeng Chen. 3d-aware indoor scene synthesis with depth priors. 2022. 2
- [35] Alon Shoshan, Nadav Bhonker, Igor Kviatkovsky, and Gérard Medioni. GAN-control: Explicitly controllable GANs. In *Int. Conf. Comput. Vis.*, 2021. 2
- [36] Nurit Spingarn-Eliezer, Ron Banner, and Tomer Michaeli. GAN steerability without optimization. In *Int. Conf. Learn. Represent.*, 2021. 2
- [37] Ryohei Suzuki, Masanori Koyama, Takeru Miyato, Taizan Yonetsuji, and Huachun Zhu. Spatially controllable image synthesis with internal representation collaging. *arXiv preprint arXiv:1811.10153*, 2018. 2
- [38] Andrey Voynov and Artem Babenko. Unsupervised discovery of interpretable directions in the GAN latent space. In *Int. Conf. Mach. Learn.*, 2020. 2
- [39] Bin Xu and Carlos R. Ponce. The geometry of deep generative image models and its applications. In *Int. Conf. Learn. Represent.*, 2021. 2
- [40] Yuxiang Wei, Yupeng Shi, Xiao Liu, Zhilong Ji, Yuan Gao, Zhongqin Wu, and Wangmeng Zuo. Orthogonal jacobian regularization for unsupervised disentanglement in image generation. In *Int. Conf. Comput. Vis.*, 2021. 2
- [41] Zongze Wu, Dani Lischinski, and Eli Shechtman. StyleSpace analysis: Disentangled controls for StyleGAN image generation. In *IEEE Conf. Comput. Vis. Pattern Recog.*, 2021. 2
- [42] Yinghao Xu, Sida Peng, Ceyuan Yang, Yujun Shen, and Bolei Zhou. 3d-aware image synthesis via learning structural and textural representations. In *IEEE Conf. Comput. Vis. Pattern Recog.*, 2022. 2
- [43] Yinghao Xu, Yujun Shen, Jiapeng Zhu, Ceyuan Yang, and Bolei Zhou. Generative hierarchical features from synthesizing images. In *IEEE Conf. Comput. Vis. Pattern Recog.*, 2021. 2
- [44] Ceyuan Yang, Yujun Shen, Yinghao Xu, Deli Zhao, Bo Dai, and Bolei Zhou. Improving gans with a dynamic discriminator. *Adv. Neural Inform. Process. Syst.*, 2022. 2
- [45] Ceyuan Yang, Yujun Shen, and Bolei Zhou. Semantic hierarchy emerges in deep generative representations for scene synthesis. *Int. J. Comput. Vis.*, 2020. 1, 2
- [46] Fisher Yu, Ari Seff, Yinda Zhang, Shuran Song, Thomas Funkhouser, and Jianxiong Xiao. LSUN: Construction of a large-scale image dataset using deep learning with humans in the loop. *arXiv preprint arXiv:1506.03365*, 2015. 4, 5
- [47] Oğuz Kaan Yüksel, Enis Simsar, Ezgi Gülperi Er, and Pinar Yanardag. LatentCLR: A contrastive learning approach for unsupervised discovery of interpretable directions. In *Int. Conf. Comput. Vis.*, 2021. 2
- [48] Yuxuan Zhang, Huan Ling, Jun Gao, Kangxue Yin, Jean-Francois Lafleche, Adela Barriuso, Antonio Torralba, and Sanja Fidler. DatasetGAN: Efficient labeled data factory with minimal human effort. In *IEEE Conf. Comput. Vis. Pattern Recog.*, 2021. 2
- [49] Bolei Zhou, Hang Zhao, Xavier Puig, Tete Xiao, Sanja Fidler, Adela Barriuso, and Antonio Torralba. Semantic understanding of scenes through the ade20k dataset. *Int. J. Comput. Vis.*, 2018. 4
- [50] Jiapeng Zhu, Ruili Feng, Yujun Shen, Deli Zhao, Zhengjun Zha, Jingren Zhou, and Qifeng Chen. Low-rank subspaces in GANs. In *Adv. Neural Inform. Process. Syst.*, 2021. 1, 2, 3, 4
- [51] Jiapeng Zhu, Yujun Shen, Yinghao Xu, Deli Zhao, and Qifeng Chen. Region-based semantic factorization in GANs. In *Int. Conf. Mach. Learn.*, 2022. 1, 2, 7, 8, 11, 12, 13
- [52] Jun-Yan Zhu, Philipp Krähenbühl, Eli Shechtman, and Alexei A Efros. Generative visual manipulation on the natural image manifold. In *Eur. Conf. Comput. Vis.*, 2016. 2, 7

Appendix

This paper proposes LinkGAN that explicitly links some latent axes to a region of an image or a semantic by utilizing an easy yet powerful regularizer. The Appendix is organized as follows. We first give the implementation details of our method in Appendix A. Second, we give an ablation study on whether or not to use the discriminator on the perturbed images in Appendix B. Third, more comparison results with other methods are given in Appendix C to show the advantages of our method.

A. Implementation Details

We use the [official Pytorch implementation](#) of StyleGAN2 [20] and [official Pytorch implementation](#) of EG3D [4] to validate our method. We keep all the parameters untouched except our newly added regularizer during training. For FID, we directly follow the original codebase, and for the masked MSE, we computed it on 10,000 images for each edit. For the update frequency of our lazy regularization, we calculate once every 8 minibatches. For how many axes we use to control the specific region, we list as below: 1). For small regions, we use 64 axes, such as the eye, nose, mouth, and ear region on FFHQ or AFHQ. 2). For the larger region, such as the left region of the human face and the bottom part of the church in Fig.3 of the main text, we use 128 axes. Also, for tokenized control in Fig.5 of the main text, each part has a size of 128 since we evenly spilt the latent codes. 3). When the partition size becomes bigger, such as half of the image, we use 256 axes, and for the semantic control (church, sky, and car) in Fig.4 of the main text, we use 256 axes as well. For the loss weight λ_1 and λ_2 , we list as below: 1). For the latent segment with 64 axes, we set λ_1 equal to 0.01 and λ_2 equal to 0.04. 2). For the latent segment with 128 axes, we set λ_1 equal to 0.01 and λ_2 equal to 0.03. 3). For the latent segment with 256 axes, we set λ_1 equal to 0.01 and λ_2 equal to 0.01.

B. Ablation Study

Here we conduct an ablation study, that is, whether or not to use the discriminator on the perturbed images. And we do the study on the eye region of AFHQ [6] dataset. Fig. 9 gives some abnormal random perturbed results on the eyes region without involving the discriminator on the perturbed images during training, from which we can discover some unrealistic perturbation. For instance, the eyes of the first cat are distorted, which can not be in the real image, and the eyes of the second cat turn to be dog eyes. Also, the leopard feature appears when perturbing the dog’s eyes. Hence, in such cases, we need to involve the discriminator in those perturbed images to hinder the generator from synthesizing those unrealistic perturbed images.



Figure 9. Ablation study on AFHQ [6] when not to use discriminator on the perturbed images.

C. More results

Besides the method we compare in the main text, here we compare our method with the baseline StyleCLIP [27], which can use text to control the synthesized images. We also provide the comparison results with ReSeFa [51]. Fig. 10 gives the comparison results on opening eyes, for LinkGAN and ReSeFa [51], we posteriorly discover semantics that can change eye size. For StyleCLIP [27], we use the text “extremely big eyes” for the optimization. As we can see from Fig. 10, StyleCLIP can successfully make the eyes bigger. However, the global color of the edited images is easily changed, such as the first column shows in Fig. 10. Fig. 11 shows the comparison results on the opening mouth, for LinkGAN and ReSeFa [51], we also posteriorly discover semantics that can open the mouth of a face image. For StyleCLIP, we use the text “open mouth” for the optimization. As shown in Fig. 11, StyleCLIP also suffers from the global change of the image when editing a specific region. For instance, the identity of the man changed in the third column, and the background of the man in the six column varied. On the contrary, our LinkGAN achieves much more precise control of the local region thanks to our explicit link.

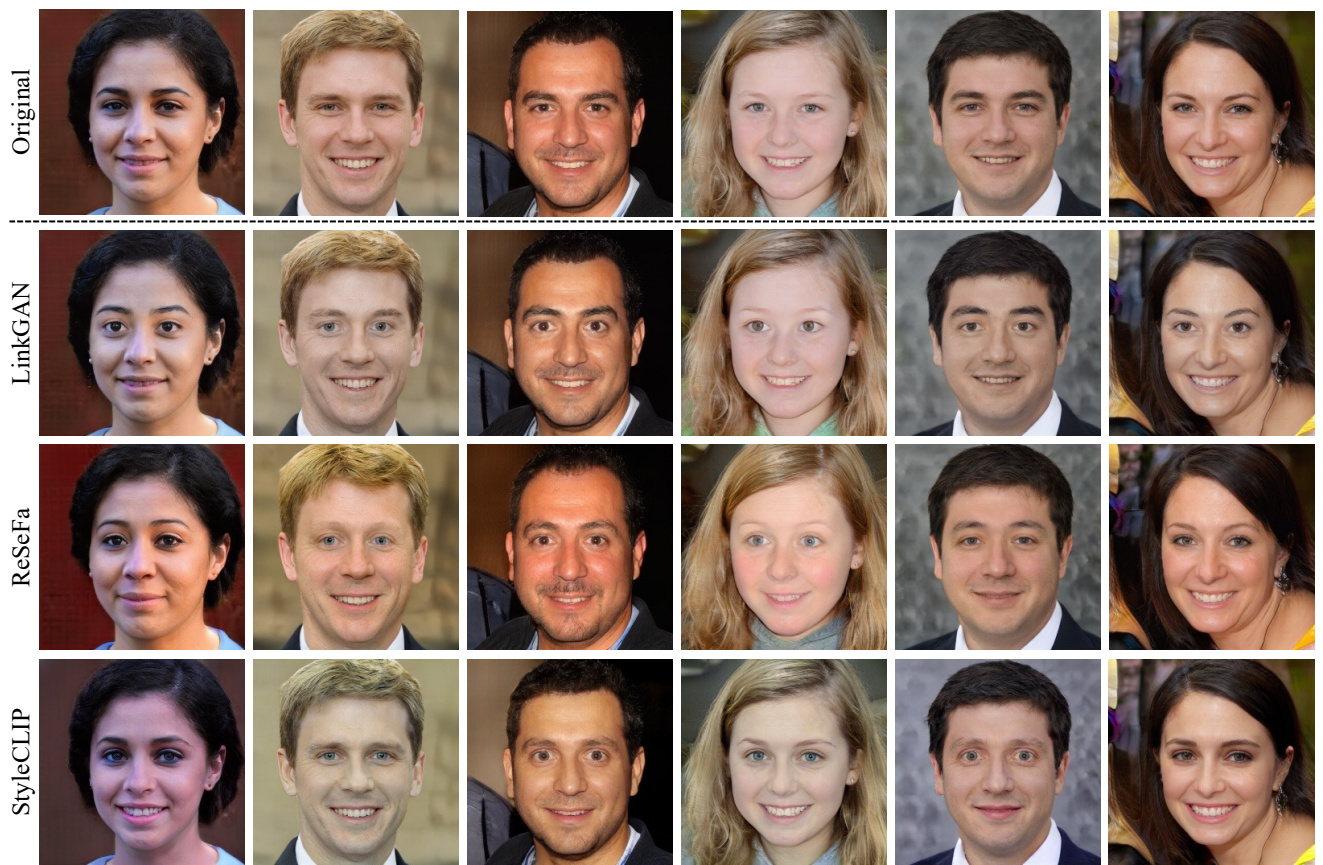


Figure 10. **Qualitative comparison** on eyes with ReSeFa [51] and StyleCLIP [27]. LinkGAN achieves more precise control within the regions of interest.

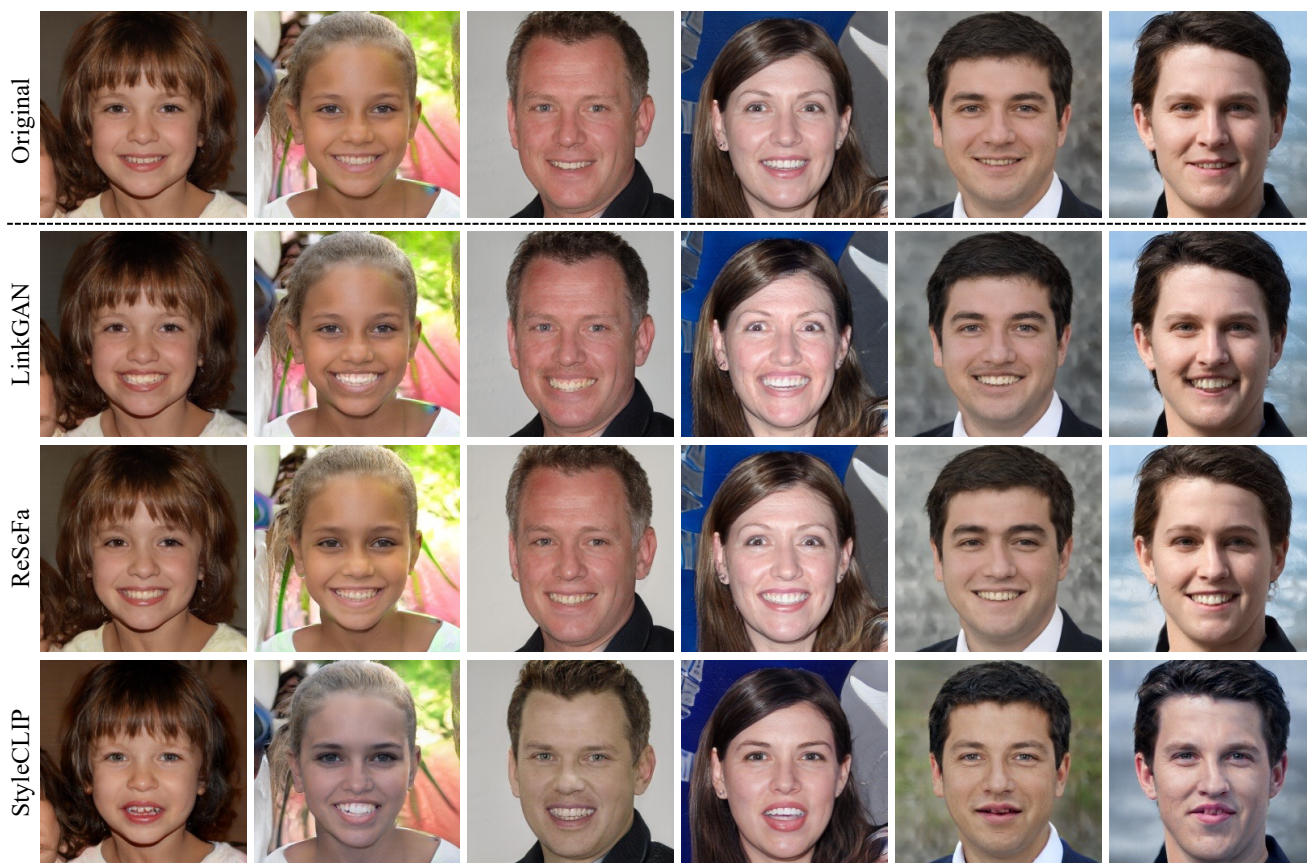


Figure 11. **Qualitative comparison** on mouth with ReSeFa [51] and StyleCLIP [27]. LinkGAN achieves more precise control within the regions of interest.